



## Research article

# Monitoring and predicting development of built-up area in sub-urban areas: A case study of Sleman, Yogyakarta, Indonesia

Nursida Arif<sup>a,b,\*</sup>, Laras Toersilawati<sup>b</sup><sup>a</sup> Department of Geography Education, Universitas Negeri Yogyakarta, Yogyakarta, 55281, Indonesia<sup>b</sup> National Research and Innovation Agency (BRIN), Bandung, 40135, Indonesia

## ARTICLE INFO

## Keywords:

Built-up area  
CA-Markov  
Land surface temperature  
Satellite imagery

## ABSTRACT

Monitoring built-up areas in the previous year and possible predictions for the following year are important in planning regional development and controlling the expansion of built-up areas. This study detects changes in the built-up area (2018–2022). It predicts the future (2026) using Landsat satellite imagery in the Sleman Regency, Yogyakarta Special Region, Indonesia study area. Mapping built-up areas is identified using the Normalized Difference Built-Up Index (NDBI). Vegetation conditions were analyzed using the Normalized Difference Vegetation Index (NDVI). Changes in the built-up area are predicted using the CA-Markov chain model for 2026. The prediction is calibrated by comparing the simulated map with the results of the classification of built-up areas in 2022. The research findings show that the built-up area has increased by 12.84 % from 2018 to 2022 and is predicted to increase by 15.48 % in 2026. The existence of built-up areas has an influence on land surface temperatures where the analysis results show a moderate correlation between NDBI and LST, namely 2018 ( $R^2 = 0.401$ ), 2019 ( $R^2 = 0.323$ ), 2020 ( $R^2 = 0.401$ ), 2021 ( $R^2 = 0.415$ ), and 2022 ( $R^2 = 0.384$ ). The higher the NDBI value, the higher the LST value, and vice versa. Therefore, regional development planning, mainly built-up areas, is an important recommendation for decision-makers in the study area.

## 1. Introduction

Urbanization raises resource and environmental problems due to increased population and built-up area while also causing an increase in urban heat islands (UHI), which impact the surrounding area. Urbanization is expected to cause land surface temperatures in most parts of the world, especially in developing countries, to increase exponentially (Kikon et al., 2016). Rapid urban development has transformed large areas of vegetation cover into impermeable surfaces, profoundly changing the atmospheric and climatic conditions in urban areas [1,2]. Increased temperature and heat increase the demand for cooling, resulting in the transfer of excess heat and moisture to the atmospheric air, which can threaten the health of the occupants in the long term. Anthropogenically induced loss of vegetation cover increases built-up and impervious surfaces in urban areas, resulting in changes in monthly and annual average temperatures. Monitoring the development of built-up area in urban areas is useful for seeing very dynamic urban development.

The study area, Sleman Regency, is part of the Special Region of Yogyakarta Province, an educational and tourism city in Indonesia. The student population in Yogyakarta makes up around 20 % of the city's total population, most of whom come from other parts of Indonesia [3]. As a tourist city, Yogyakarta has worldwide tourist attractions: natural, cultural, and unique [3,4]. In recent years

\* Corresponding author. Department of Geography Education, Universitas Negeri Yogyakarta, Yogyakarta, 55281, Indonesia.  
E-mail address: [nursida.arif@uny.ac.id](mailto:nursida.arif@uny.ac.id) (N. Arif).

<https://doi.org/10.1016/j.heliyon.2024.e34466>

Received 5 October 2023; Received in revised form 30 June 2024; Accepted 10 July 2024

Available online 14 July 2024

2405-8440/© 2024 The Authors. Published by Elsevier Ltd. This is an open access article under the CC BY-NC-ND license (<http://creativecommons.org/licenses/by-nc-nd/4.0/>).

tourism in Yogyakarta has been overgrown, and Sleman is no exception [5]. The presence of many tourists requires expanding built-up areas to accommodate more tourists [6], thus encouraging land conversion for tourism development [7]. It is one of the causes of the relatively high intensity of the increase in built-up areas in Sleman during 2005–2015 [8]. Geographically, Sleman Regency is considered a provider of most of the water in Yogyakarta because of its location in the upstream part of Yogyakarta [9]. The future spatial pattern of built-up area use will affect water supply-demand risks [10]. Therefore, monitoring and predicting built-up area in the future is very important in Sleman Regency for regional development planning that considers ecological conditions.

Remote sensing can support reliable and effective monitoring systems. In recent years, technology has solved the problem of spatial big data analysis, such as time series data. Google Earth Engine (GEE) is one of the most widely used. This geospatial analysis platform allows users to visualize and analyze imagery for free at large sizes down to the petabyte scale [11]. Users can access and analyze data from the public catalog and their private data using the operator library provided by the Earth Engine API [12]. Several studies have conducted using GEE, such as real-time mapping of urban built-up areas [13], extraction of buildings in urban areas [14], land cover classification [15], and mapping temporal Normalized Difference Vegetation Index [16].

Satellite imagery can detect land surface changes based on several vegetation indices often used in the environmental domain, including land surface temperature and vegetation index transformation [17,18]. NDVI is a vegetation index transformation widely used for monitoring vegetation [19–21]. Several previous studies have shown that the relationship between NDVI and soil surface moisture has a strong positive correlation [20,22]. Land change, increase in urban settlements, and other anthropogenic activities increase surface temperature. LST is a condition controlled by the surface and subsurface media’s balance of surface energy, atmosphere, and thermal properties [23–26]. Generally, green vegetation and water bodies indicate low LST, while built-up areas, bare land, or dry land reflect high LST. In addition to vegetation and surface temperature, it is important to analyze built-up areas to see the spatial dynamics of built-up area development in cities. Several previous researchers relied on NDBI for the analysis of built-up areas [27–29]. NDBI can be useful in identifying rapid urban growth and the conversion of agricultural and forest land into low-density development. It is an objective measure that can provide valuable insights into land use changes [29]. NDBI found to have a strong correlation with LST and NDVI [30,31].

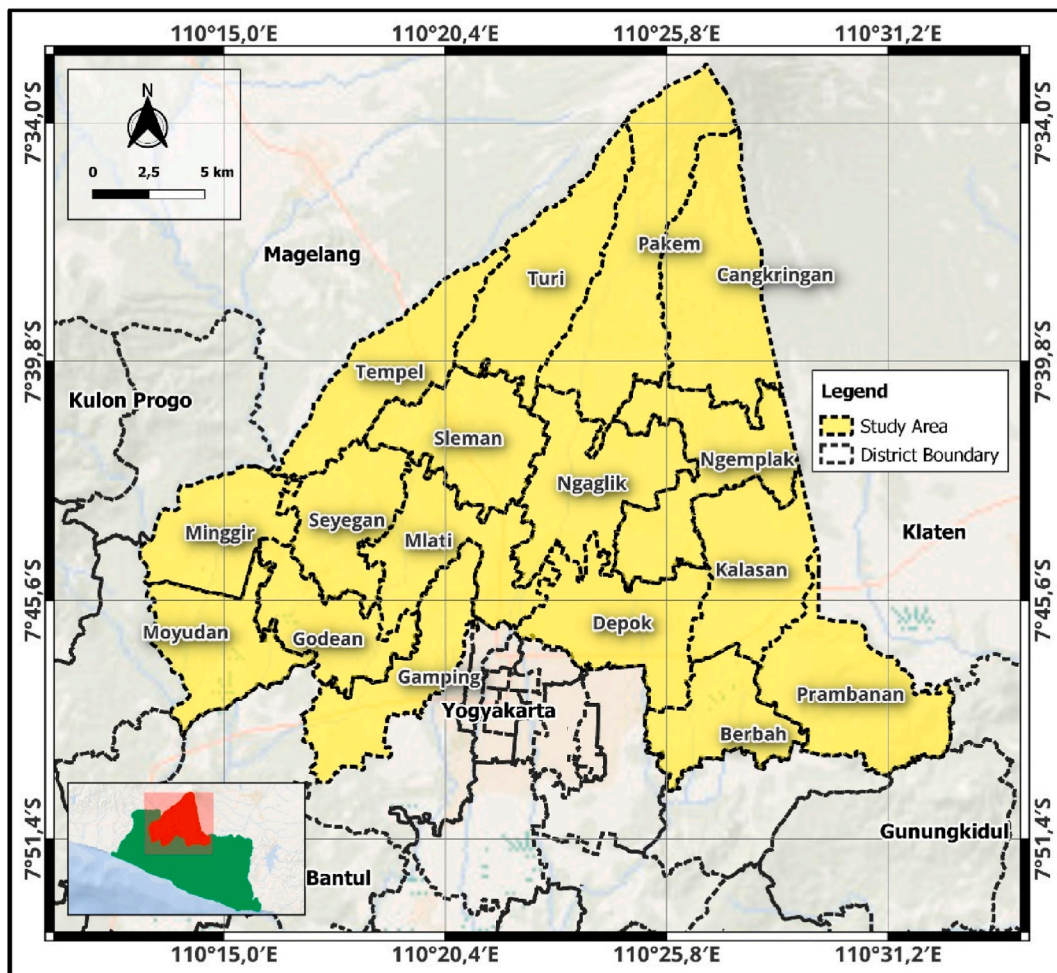


Fig. 1. Map of research location (Sleman regency) [36].

The reliability of remote sensing and geographic information systems can assist spatial changes in an area, including built-up areas. Cellular Automata and Markov Chain (CA-Markov) are widely used to make good predictions [32]. Several studies have been conducted in various regions to analyze past, present, and future land use changes using CA-Markov [33–35]. This model helps policy-makers make rational decisions in the region’s development. Therefore, the main objective of this research is to analyze the spatiotemporal changes of the built-up area over five years (2018–2022) and to predict the built-up area in 2026 using the CA-Markov spatial modeling.

## 2. Materials and methods

### 2.1. The study area

The investigation is being conducted in Sleman Regency, a district in Yogyakarta, Indonesia’s Special Region. Its geographical coordinates are 110°33’00” to 110°13’00” East Longitude and 7°34’51” to 7°47’30” South Latitude (Fig. 1). Sleman is a district with very dynamic and fast changes, with a high level of urbanization and a dynamic increase in built-up area [8].

The northern part of Sleman district is rich in water resources due to its location on the slopes of Mount Merapi, starting from the road that connects the districts of Tempel, Turi, Pakem, and Cangkringan up to the peak of Mount Merapi. The eastern area is home to historical heritage (temple) covering the Prambanan District, parts of Kalasan District, and Berbah District. The middle region is the agglomeration area with the city of Yogyakarta, including the Districts of Mlati, Sleman, Ngaglik, Ngemplak, Depok, and Gamping. The western region is a wetland agricultural area with sufficient water and a source of raw materials for craft industry activities in the Districts of Godean, Minggir, Sayegan, and Moyudan.

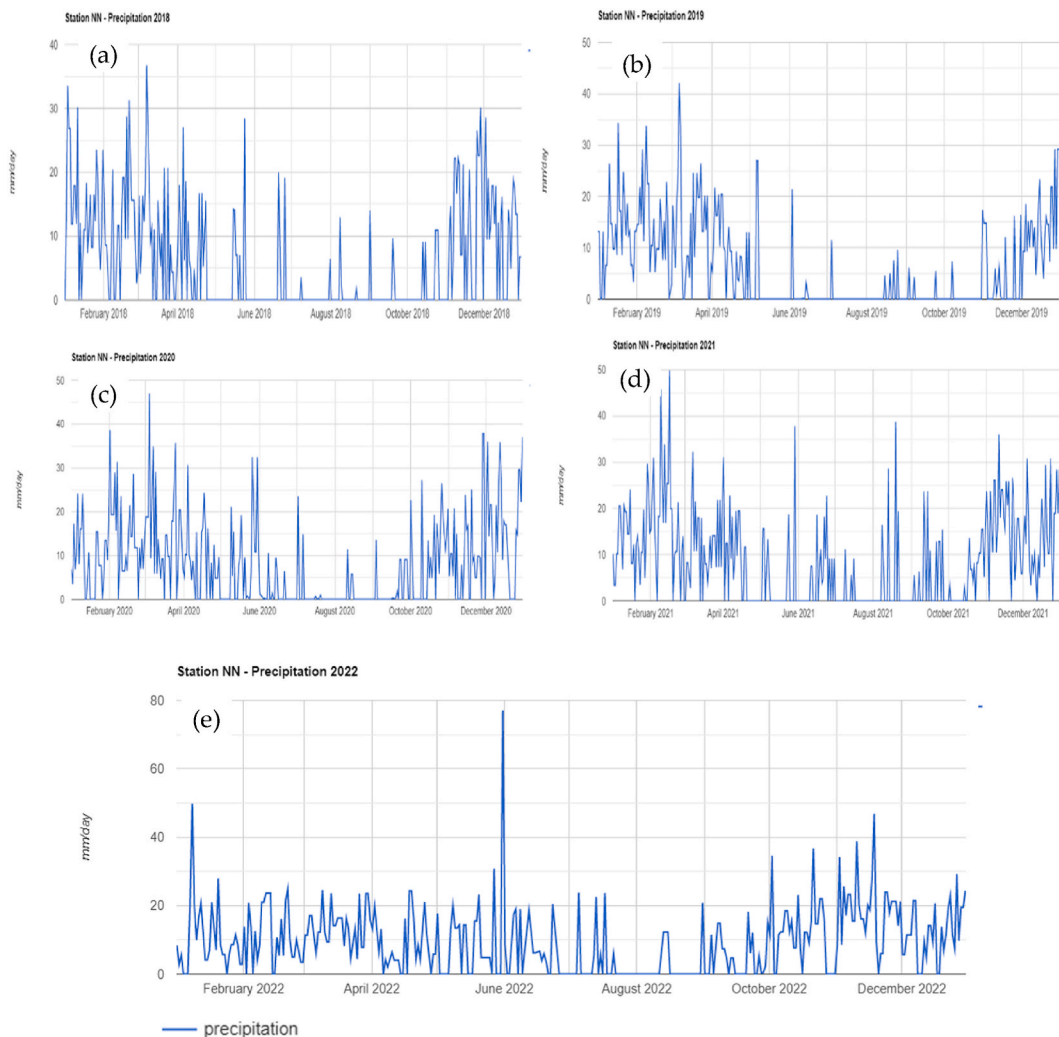


Fig. 2. Annual precipitation in Sleman regency in 2018–2022 (a) 2018; (b) 2019; (c) 2020; d (2021); e (2022)

Sleman Regency experiences a wet tropical climate with a rainy season between November–April and a dry season between May–October, as shown by the rainfall data obtained from CHIRPS (<https://data.chc.ucsb.edu/>) during the period 2018–2022 (Fig. 2a–e). Fig. 2a–e shows the same pattern where rainfall is high in December–April and begins to decrease in May–November. The difference is only in the intensity of rainfall, as shown in Fig. 2b; precipitation fluctuation decreases in October–December. Likewise, in 2022 (Fig. 2e), the average CH intensity is < 40 mm/day except for August, which is < 20 mm/day. This is per the predictions that in 2022 the atmosphere and oceans will experience significant changes culminating in different weather patterns. Ocean temperatures and pressure patterns during La Nina will result in stable conditions and less rainfall [37].

## 2.2. Methodological approach and datasets

Imagery analysis is performed on GEE by filtering and masking with 20 % cloud cover on Landsat 8 and 9 imagery. Filtering operations are performed annually on the best imagery collection for five years of data. The 2018–2020 imagery dataset uses Landsat 8 with the script: ee.ImageCollection("COPERNICUS/S2\_SR\_HARMONIZED"). The 2021 and 2022 datasets use Landsat 9 imagery with the script ee.ImageCollection("LANDSAT/LC09/C02/T1\_L2"). The timeframe considered for this analysis is from year to year, and annual collections are made based on the average values of the NDVI, NDBI, and LST indices. The government website confirmed LST data with secondary population density data (<https://slemankab.bps.go.id/>, accessed on June 5, 2023). The Flowchart in Fig. 3 illustrates the stages of data processing.

Linear regression method (LR) is used to approximate the independent variable reported on the value or change in other variables studied in linear shape [38]. LR is very appropriate for seeing the correlation between two variables [39].

### 2.2.1. NDVI, NDBI, and LST

The Normalized Difference Vegetation Index and Normalized Difference Built-up Index are valuable tools in monitoring urban development. NDBI is used to identify built-up areas, and is proven to have a positive linear relationship with surface temperature and a negative correlation with NDVI [40]. A high NDBI indicates a larger proportion of built-up area, reflecting urban development and land use changes [41]. The combination of NDVI and NDBI can provide a dynamic picture of urban growth and land use change, making it valuable for assessing spatio-temporal urban growth, land use land cover change, and the environmental impacts of rapid urbanization [29].

Likewise LST is a valuable tool for monitoring urban development. LST measurements can be used to assess the sustainability of urban growth, monitor temperature patterns over time, and identify areas vulnerable to heat stress, such as densely populated urban areas or regions with high agricultural activity [42,43]. Dalam sebuah penelitian rata-rata LST 28,74 °C untuk kawasan terbangun [44]. The various index formulas used in this study are presented in Table 1.

### 2.2.2. CA-Markov Chain

This study's prediction process for built-up areas was determined using the CA-Markov chain model. Markov chain is a stochastic process that experiences transitions from one state to another according to the state space [34]. CA is a mathematical model that shows how different elements in time change dramatically under the influence of nearest-neighbor values. CA-Markov is a mixed model between knowledge-based cellular automata integrated with Markov chains and spatiotemporal dynamic modeling. A Markov chain creates a set of probability values that indicate the probability of changing the user interface over a certain period, depending on the

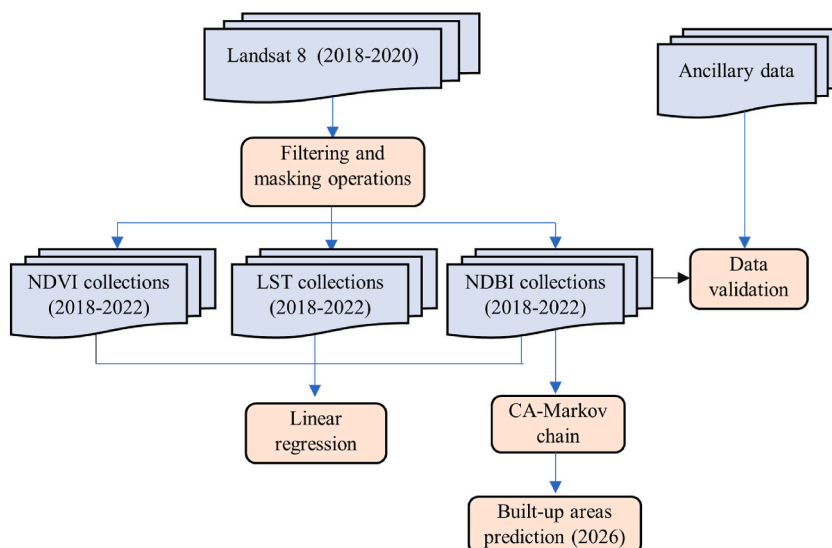


Fig. 3. Flowchart of built-up area prediction methodology.



**Table 1**  
The equation used for NDVI, NDBI, and LST calculations.

Index Name	ID Index	Band Used	Formulas	Application	References
Normalized different vegetation index	NDVI	near infra red (nir), red	$\frac{nir - red}{nir + red}$	mapping vegetation cover	[45]
Normalized different built-up index	NDBI	short wave infrared (swir) and nir	$\frac{swir - red}{swir + red}$	automatically mapping urban areas.	[46]
Land Surface Temperature index	LST	thermal infrared sensor (TIRS-1), TIRS-2	$T_s = \frac{K_2}{\ln\left(\frac{\epsilon NB K_1}{R_c} + 1\right)}$	mapping land surface temperatures	[47]

number of changes in the past [32]. This research simulated IDRISI software that developed a land use change model. This model consists of two main stages: (1) calculating the probability of conversion, including the conversion probability matrix using Markov chain analysis, and (2) simulating the spatial specifications of land use based on CA operators and multi-criteria evaluation (MCE).

### 3. Results

#### 3.1. Spatial distribution of NDVI, NDBI, LST

The results of the NDVI analysis over five years (2018–2022) are presented in Fig. 4a- 10e with the maximum average ranging from (0.8–0.9) while the average minimum value range from (–0.12) – (–0, 30). Over five years, the NDVI values have almost the same range, namely 2018 (Fig. 4a,-0.12 – 0.81), 2019 (Fig. 4b,-0.24 – 0.88), 2020 (Fig. 4c–0.24 -0.91), 2021 (Fig. 4d,-0.30-0.89), 2022 (Fig. 4e–0.28-0.90). Variations in NDVI values and vegetation indices indicate changes in current vegetation dynamics and trends [39].

Fig. 4a–e shows the highest NDVI values spatially distributed in the northern region, while the lowest NDVI values dominate the southern region where land cover is mainly built-up area. Differences in NDVI values over built-up areas based on the testing of several

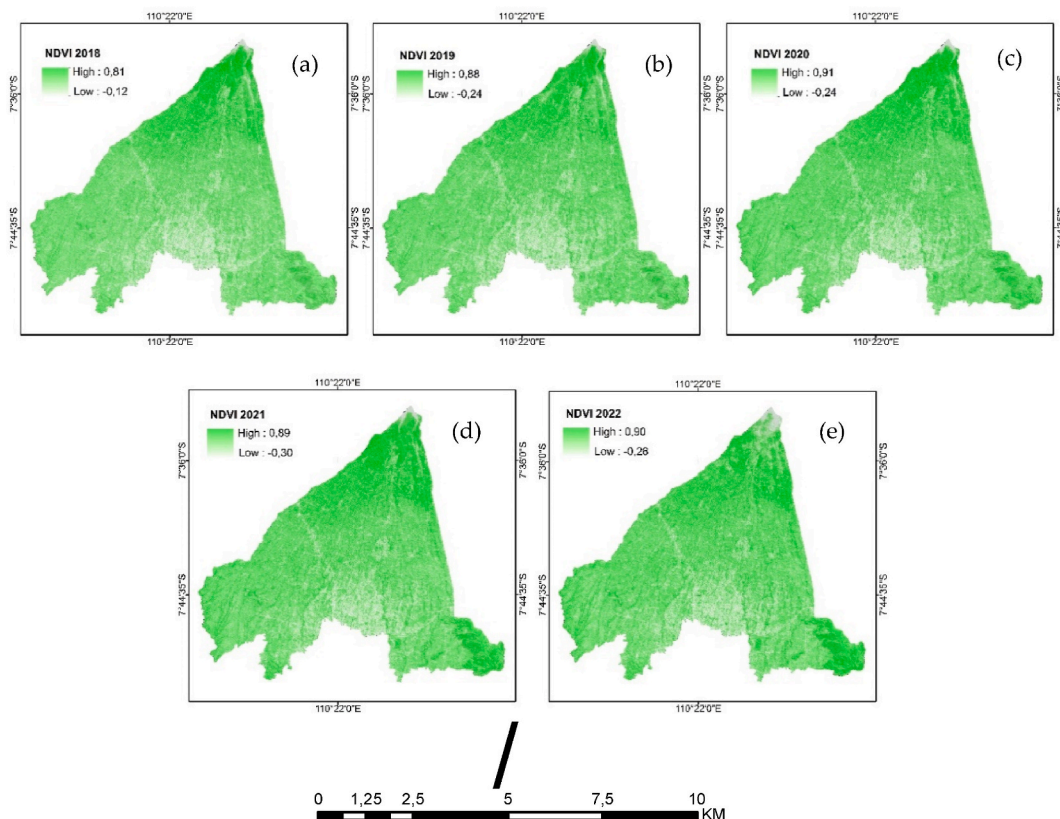


**Fig. 4.** Spatial distribution of NDVI in Sleman regency in 2018–2022: (a) 2018; (b) 2019; (c) 2020; (d) 2021; (e) 2022.

samples are presented in Table 3.

Table 2 shows the NDVI values over built-up land, and the peak of Mount Merapi is lower than the NDVI value over vegetated areas. Built-up land provides a reflection that contrasts with NDVI values in vegetation. However, the weakness of NDVI is that it is only specific to vegetation. It is, therefore difficult to distinguish built-up land from open land. To analyze built-up land, it is noticeable based on the NDBI results as presented in Fig. 5.

Fig. 5 shows the NDBI values did not differ significantly during 2018–2022; namely the lowest values ranged from (−0.44) – (−0.56). That the NDBI values did not differ significantly between 2018 and 2022, namely, the lowest values ranged from (−0.44) – (−0.56). While the highest values ranged from (0.38–0.45). NDBI values < 0 can extract water bodies, while NDBI >0.1 can extract built-up areas and bare land [23]. This study took samples from different land cover types to observe the NDBI values during 2018–2022 (Fig. 6).

Fig. 6 shows the NDBI values for vegetation, namely 2018 (−0.31), 2019 (−0.19), 2020 (−0.32), 2021 (−0.33), and 2022 (−0.34). Whereas the NDBI values for built-up - 1 land are 2018 (0.10), 2019 (0.16), 2020 (0.18), 2021 (0.06), and 2022 (0.13). On built-up - 2 land, namely 2018 (0.07), 2019 (0.18), 2020 (0.15), 2021 (0.07), 2022 (0.09). In other studies, its also written that the average built-up area ranges from 0.1 to 0.3 [48]. The NDBI value used to classify and predict built-up land in the future, namely the periods of 2018, 2022, and 2026 with the results obtained that built-up area continues to increase (Table 3 and Fig. 7). The map of the predicted built-up areas in 2026 is presented in Fig. 7.

Fig. 7 shows the spatial distribution of built-up area in 2026, where the built-up areas are clustering in the southern part of the study area, namely in the sub-districts of Depok, Mlati, and Ngaglik, as well as in parts of the sub-districts of Godean and Kalasan. Based on Table 3, the built-up area increase by 11.28 km2 in 2022, and it is predicted to increase by 13.52 km2 in 2026.

The dynamics of land surface temperature have been seen based on LST values during 2018–2022, and the results show that the LST distribution (Fig. 5) has the same spatial pattern as the NDBI (Fig. 8a–e). LST’s maximum value spreads over the southern part of the study area. In contrast, the minimum value distributes in the northern region. The highest LST values in each year, i.e., 2018 (28.56 °C), 2019 (28.59 °C), 2020 (28.53 °C), 2021 (26.48 °C), 2022 (27.18 °C). While the lowest LST values, i.e., 2018 (21.27 °C), 2019 (21.89 °C), 2020 (20.53 °C), 2021 (20.38 °C), 2022 (19.12 °C). The highest LST scatters in the southern region, such as in the sub-districts of Gamping, Mlati, Ngaglik, and Depok. The four sub-districts have the highest LST values due to the high population in the area (Table 4).

### 3.2. LST, NDBI, and NDVI correlation

Fig. 9a–e shows the correlation between NDBI and LST. Correlation points indicate the number of samples tested (n = 666). The higher the NDBI value, the higher the LST value, and vice versa. A relatively low correlation occurred in 2019 and 2022 (Fig. 9b and e), and this means that the NDBI can be sufficiently used to describe the level of built-up land. The difference in correlation values is due to the difference between the image recording time for the image used to extract LST values and the average conditions of the image used to analyze NDBI. Fig. 10a–e shows the LST and NDVI correlations.

A relatively weak correlation between LST and NDVI occurs in 2022 (Fig. 10e), namely  $R^2 = 0.269$ , while 2018–2021 has a moderate correlation (Fig. 10a–d). Based on these results, it can be concluded that the NDVI values have a negative correlation with the LST values, whereas areas with low NDVI values have a high LST value.

## 4. Discussion

This study uses the NDBI to monitor urban development for five years (20018-2022) to ascertain the condition of built-up land. The results show no significant changes in Sleman districts during this period (Fig. 5a–e), although the test results from several sample points showed an increase in the NDBI value for 5 years (Fig. 7). The NDBI value fluctuates over time, influenced by changes in the built-up area and the extent of bare land within the study area. The fluctuations in NDBI values over time can be attributed to the conversion of land use from vegetated areas to built-up areas and vice versa. Conversely, an increase in vegetation will result in a fall in the NDVI value, thereby indicating a higher proportion of vegetation [30]. It is difficult to quickly analyze temporal variations in urban dynamics based solely on built-up land conditions [50]. However, this paper is sufficient to show the relationship between built-up land and LST by extracting NDBI values. NDBI is a valuable indicator for forecasting the expansion of urban areas. It quantifies the density of built-up structures, including buildings, roads, and other infrastructure.

The spatial pattern of LST values in Sleman Regency shows peak values in areas with high population density (Fig. 8a–e). However, future planning for Sleman Regency has been carried out well, the population in dense areas has decreased, on the contrary, there has been an increase in population density in areas that were previously not included in the dense category (Table 4). This has a positive

**Table 2**  
NDVI values for different land cover types.

Coordinate		Landcover	NDVI-value				
X	Y		2018	2019	2020	2021	2022
0429810.602	09142729.82	built-up area	−0.02	−0.006	−0.03	−0.007	−0.01
0429983.02	09157508.31	dense vegetation	0.73	0.73	0.85	0.73	0.83
0438688.83	9166028,91	the peak of mount Merapi	−0.01	0.00	0.01	−0.02	0.03

**Table 3**  
Built-up land area of Sleman regency in 2018, 2022 and 2026.

Landuse	Area (Km <sup>2</sup> )		
	2018	2022	2026
built-up areas/bare land	81,80	93,08	106,60
non built-up area	493,01	481,72	468,20

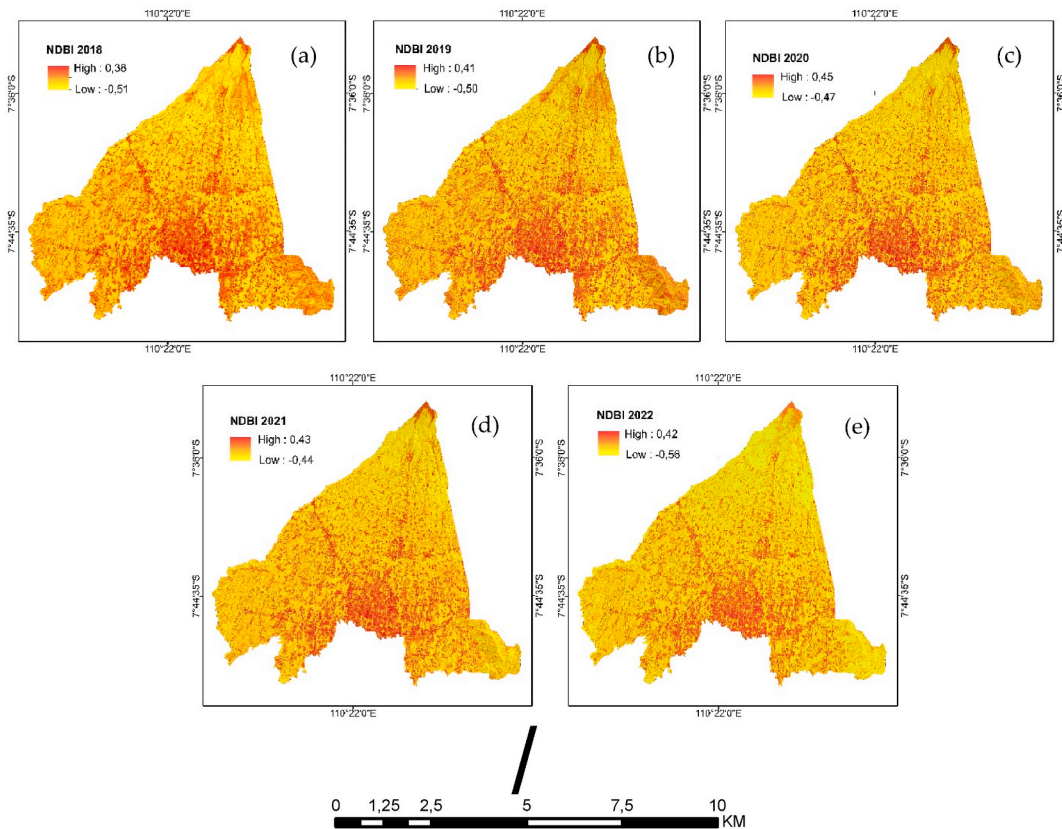


**Fig. 5.** Spatial distribution of NDBI in Sleman regency in 2018–2022: (a) 2018; (b) 2019; (c) 2020; (d) 2021; (e) 2022.

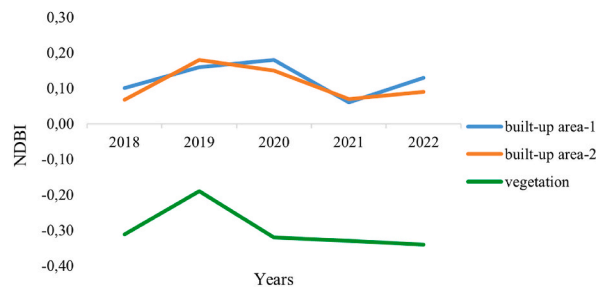


**Fig. 6.** Graph of NDBI values on vegetation land cover and built-up area.

impact on regional development, namely reducing spatial gaps in infrastructure, resources and opportunities [51]. The pattern of the NDVI values is the opposite of the LST values (Figs. 4 and 8). The high density of vegetation causes the surface temperature to be lower. Urbanization creates an inverse relationship between impermeable cover and vegetation, generating new LST patterns due to the correlation of LSTs with impermeable cover and vegetation [52]. Table 4 shows the four sub-districts with the highest population numbers, namely Gamping, Mlati, Ngaglik, and Depok, where each has a population of more than 100 thousand people. A high population density of over 2.7 thousand people/km<sup>2</sup> accompanies this high population. Therefore, the higher the population density,

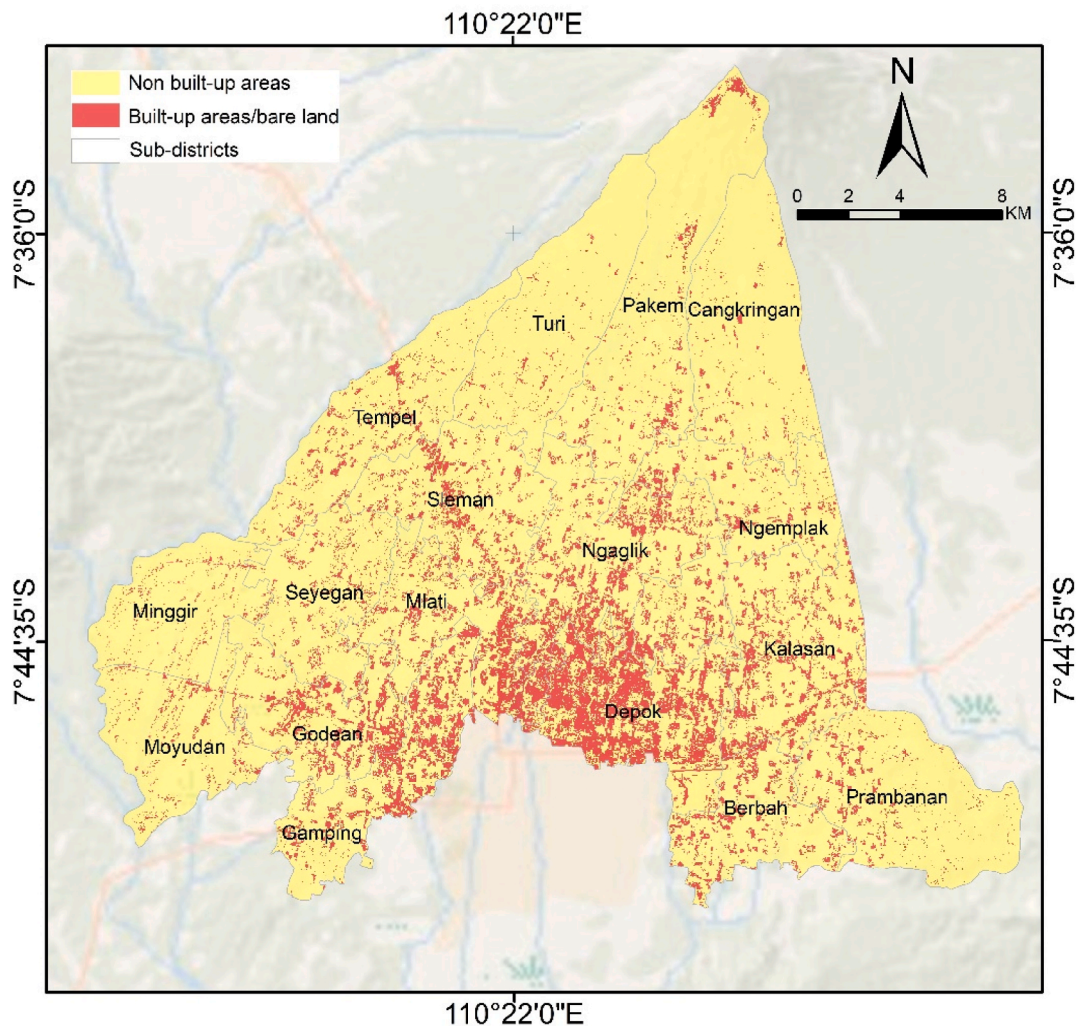


Fig. 7. Sleman district built-up area prediction map for 2026.

the higher the LST value of the area. Human-affected areas with large settlements will have higher temperatures [53].

The effects of land use, population density, and altitude on the UHI phenomenon found that LST was significantly related to population density [54]. This is consistent with the statement that population helps produce, and amplifies the harmful effects of UHI [55]. The increase in LST can also be affected by high emissivity values in urban materials such as roads [24]. The pattern of LST is the same as several previous studies where high LST is clustered in the city center, characterized with high building density and dominated by hotels and shops [56]. This paper proves that there is a moderate correlation between LST and NDBI (Fig. 9). The same pattern was conveyed by several previous researchers [30,57]. LST Distribution is confirmed by the level of greenness in the study area using NDVI. Correlation results show that NDVI has a negative correlation with LST (Fig. 10a–e). The relationship between average LST, population density, and the level of greenness in several cities has a similar spatial pattern [26,58,59]. The City density increases sensitivity to climate change [60], loss of green open space [61], and increasing urban heat islands [59,62].

The current study uses the CA-Markov chain model to detect changes in the built area in the past, present, and future. The Markov chain model can predict future land use changes [32,34]. The study's findings, including the 12.84 % increase in built-up areas from 2018 to 2022 and the predicted 15.48 % increase by 2026 (Table 3, Fig. 7), provide valuable insights for policymakers and urban planners to make informed decisions about the growth and development of the region. Several studies have shown that the prediction results of built-up areas will increase [35,63,64]. The trend of growing built-up areas in the study area could be due to urbanization and increased tourism. The increased tourism activity has put enormous pressure on destinations to develop tourism infrastructure [65]. However, future research should include an analysis of land use and land cover change assessments to provide insight into the continuously developing urban landscape [66]. For future research recommendations, NDBI is a valuable tool for monitoring the impact of greening efforts on urban development. By monitoring changes in NDBI over time, policymakers can evaluate the effectiveness of forestation initiatives in reducing urban sprawl and mitigating urban heat island impacts [67].



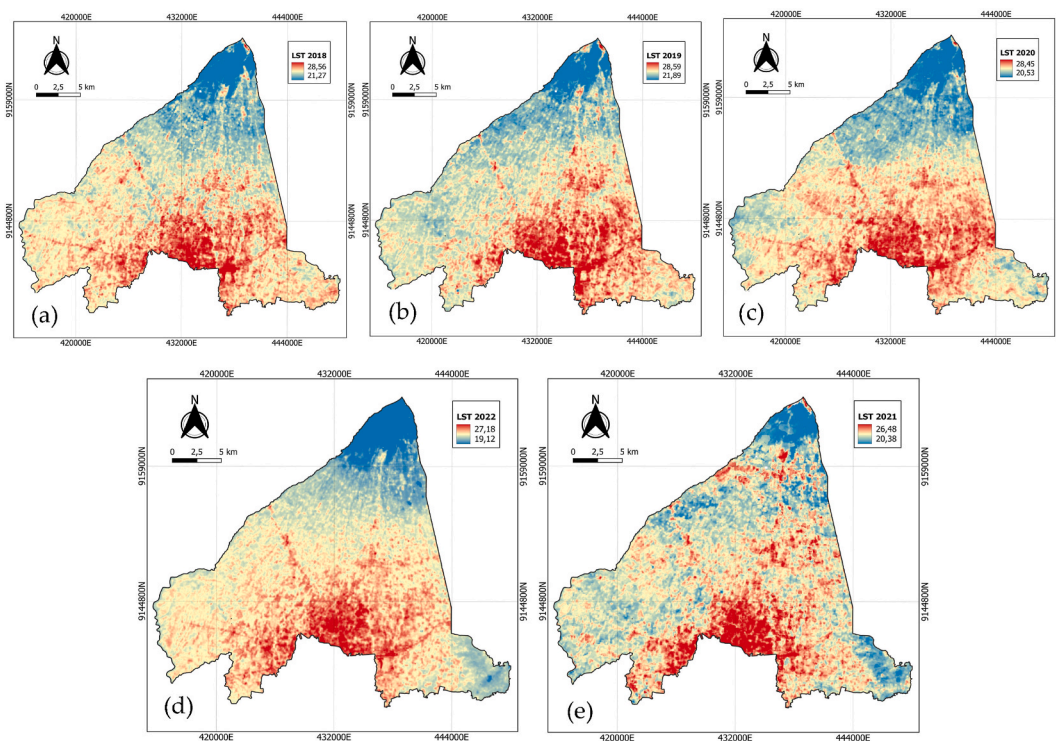


Fig. 8. Spatial distribution of LST in Sleman regency in 2018–2022: (a) 2018; (b) 2019; (c) 2020; (d) 2021; (e) 2022.

Table 4  
Population density of Sleman regency.

Subdistrict	Population Density by District (Person/KM <sup>2</sup> )					
	Total population			Population density		
	2020	2021	2022	2020	2021	2022
Moyudan	33514	33842	33684	1213.40	1225.27	1219.55
Minggir	32110	32459	32449	1177.48	1189.28	1189.92
Seyegan	51231	51967	51984	1923.81	1951.45	1952.08
Godean	72255	73036	70898	2692.06	272116	2641.50
Gamping	103192	104020	95103	3527.93	3556.24	3251.38
Mlati	100524	100707	93721	3524.68	3531.10	3286.15
Depok	131005	131242	124565	3685.09	3691.76	3503.93
Berbah	59004	59976	56449	2566.51	2608.79	2455.37
Prambanan	53113	53859	54624	1284.47	1302.52	1321.01
Kalasan	86163	87357	85210	2404.10	2437.42	2377.51
Ngemplak	67555	68576	64331	1891.77	1920.36	1801.48
Ngaglik	105612	106173	100780	2741.74	2756.31	2616.30
Sleman	71888	72972	70976	2295.27	2329.89	2266.15
Tempel	53628	54164	54739	1650.60	1667.10	1684.80
Turi	36559	36980	37914	848.43	858.20	879.88
Pakem	37320	37656	38563	851.28	858.94	879.63
Cangkringan	31131	31488	31965	648.70	656.14	666.08

Source [49]:

### 5. Conclusions

The research conducted using Landsat data to monitor LST in urban areas based on NDVI and NDBI values revealed several important findings. The highest LST value recorded was 28.59 °C in 2019, with an average of 25.25 °C. The study showed that NDBI values did not differ significantly over the last five years, ranging from −0.44 to 0.45, and the NDVI values also did not change much, ranging from −0.12 to 0.90. The research established a positive correlation between NDVI and LST, indicating that higher NDVI values are associated with lower LST values. Similarly, NDBI and LST exhibited a positive linear correlation, with higher LST values associated with higher NDBI values. The study also identified that regions with confirmed high LST are areas dominated by built-up land with a

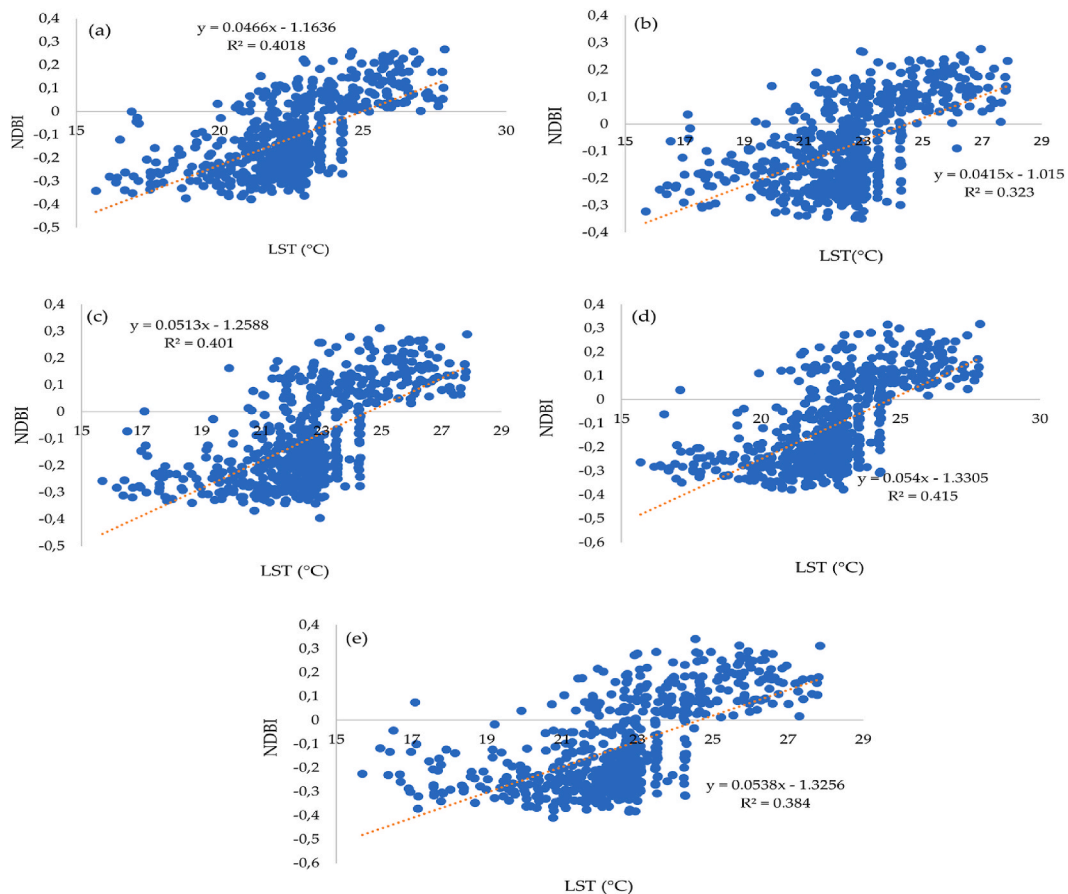


**Fig. 9.** Ndbi and LST correlation: (a) 2018; (b) 2019; (c) 2020; (d) 2021; (e) 2022.

denser population. The research concluded that the results could serve as a recommendation for environmentalists and regional planners to consider green open spaces as a counterbalance to the development of built-up areas.

The research's findings provide valuable insights into the relationship between urbanization, land surface temperature, and land use/land cover changes, and offer important implications for urban planning and environmental management. The correlations identified between LST and the NDVI and NDBI values, as well as the continued increase in built-up areas, underscore the need for well-planned urban development and the preservation of green spaces to mitigate the urban heat island effect and its associated environmental and public health impacts. The findings show that additional built-up areas in the future should be well-planned. The results of this study can be a recommendation for environmentalists and regional planners to consider green open spaces as a counterweight to the development of built-up areas.

### Funding

This research received no external funding.

### Data availability statement

To ensure transparency and reproducibility, we provide the required data and codes to replicate our findings. Interested users and researchers are encouraged to test the models for their specific use cases, while acknowledging the authors in their work. The link to the GitHub repository: <https://github.com/nursida31/predicting-development-of-built-up-area/>.

### CRedit authorship contribution statement

**Nursida Arif:** Writing – review & editing, Writing – original draft, Visualization, Supervision, Software, Methodology, Conceptualization. **Laras Toersilawati:** Writing – review & editing, Supervision, Conceptualization.

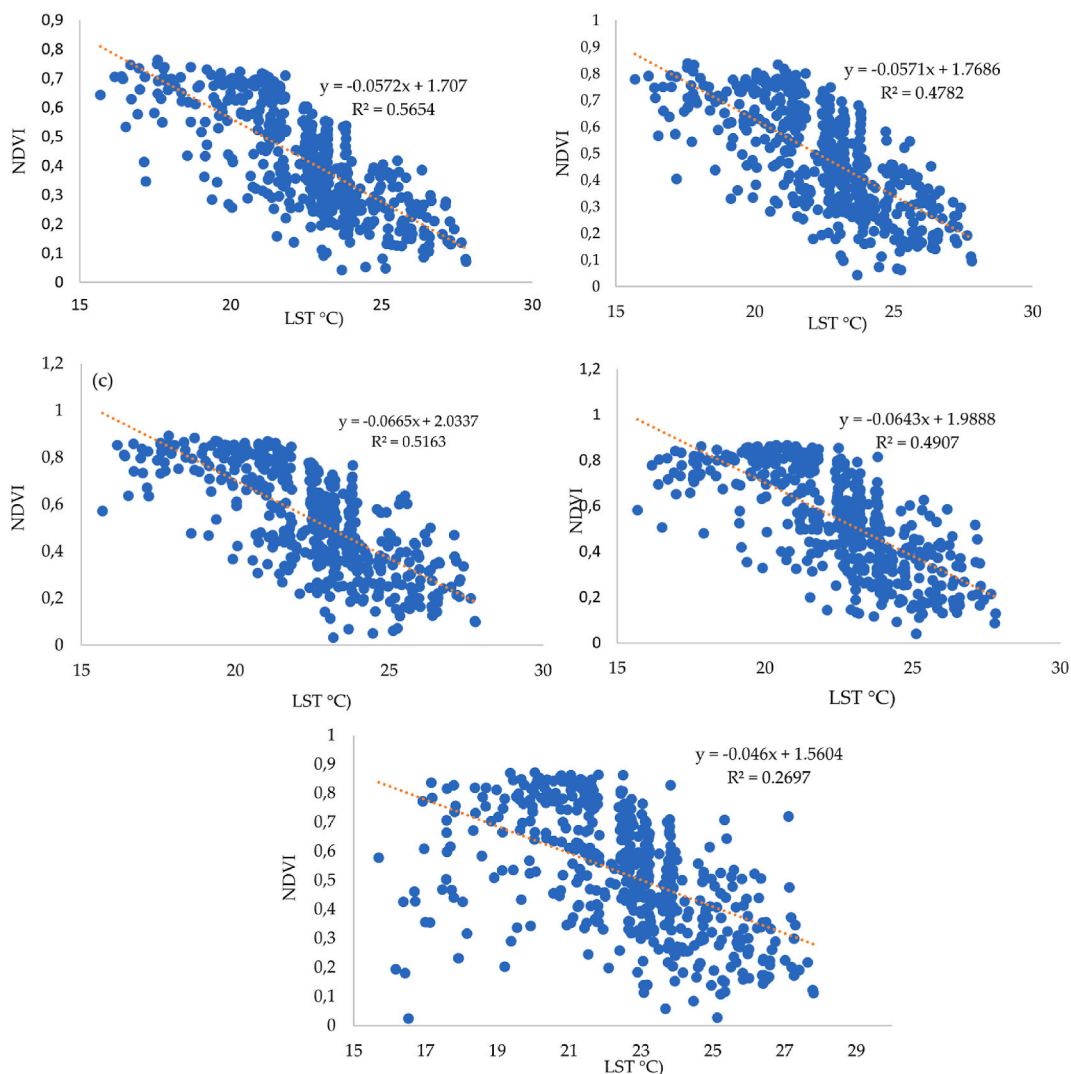


Fig. 10. Ndvi and LST correlation: (a) 2018; (b) 2019; (c) 2020; (d) 2021; (e) 2022.

**Declaration of competing interest**

The authors declare no conflict of interest.

**Acknowledgments**

The authors would like to thank the National Research and Innovation Agency (BRIN) which has provided the facilities we needed to conduct research. The authors also thank the anonymous reviewers, Sutanto Trijuni Putro, and Andrew Mullabi for beneficial comments to improv the quality of the manuscript.

**References**

- [1] W. Mu, X. Zhu, W. Ma, Y. Han, H. Huang, X. Huang, Impact assessment of urbanization on vegetation net primary productivity: a case study of the core development area in central plains urban agglomeration, China, *Environ. Res.* 229 (2023) 115995, <https://doi.org/10.1016/J.ENVRES.2023.115995>.
- [2] L. Olsson, et al., "Livelihoods and Poverty Livelihoods and Poverty Livelihoods and Poverty Climate Change 2014: Impacts, Adaptation, and Vulnerability. Part A: Global and Sectoral Aspects. Contribution of Working Group II to the Fifth Assessment Report of the Intergovernment.", Cambridge University Press, Cambridge, 2014.
- [3] T. Fleming, Cultural cities profile East Asia: Indonesia Yogyakarta (2021) 1–31, no. June, <https://tanahindie.org/>.
- [4] Syakdiah, "Dinamika pariwisata daerah istimewa Yogyakarta," *Pros. Semin. dan Call Pap.* (2017) 225–233.
- [5] Mohamad Yusuf, How far can tourism go? Residents' attitude toward tourism development in Yogyakarta city, Indonesia, *Indones. Jopurnal Geogr* 52 (2) (2020) 208–218.

- [6] F. Randelli, F. Martellozzo, Is rural tourism-induced built-up growth a threat for the sustainability of rural areas? The case study of Tuscany, *Land Use Pol.* 86 (2019) 387–398, <https://doi.org/10.1016/j.landusepol.2019.05.018>.
- [7] M.T.T. Duong, D.A.A. Samsura, E. van der Krabben, Land conversion for tourism development under vietnam's ambiguous property rights over land, *Land* 9 (6) (2020) 1–22, <https://doi.org/10.3390/land9060204>.
- [8] D. Marwasta, "The influence of Yogyakarta urban physical development to residential comfort," *KnE Soc. Sci.* 3 (5) (2018) 175, <https://doi.org/10.18502/kss.v3i5.2332>.
- [9] V. Asriningtyas, D.P.E. Putra, Ten year groundwater simulation in Merapi aquifer, Sleman, DIY, Indonesia, *Indones. J. Geogr.* 38 (1) (2006) 1–14.
- [10] X. Liu, Y. Liu, Y. Wang, Z. Liu, "Evaluating potential impacts of land use changes on water supply-demand under multiple development scenarios in dryland region," *J. Hydrol.* 610 (2022) 127811, <https://doi.org/10.1016/j.jhydrol.2022.127811>.
- [11] M. Amani, et al., "Google Earth engine cloud computing platform for remote sensing big data applications: a comprehensive review," *IEEE J. Sel. Top. Appl. Earth Obs. Remote Sens.* 13 (2020) 5326–5350, <https://doi.org/10.1109/JSTARS.2020.3021052>.
- [12] N. Gorelick, M. Hancher, M. Dixon, S. Ilyushchenko, D. Thau, R. Moore, "Google Earth engine: planetary-scale geospatial analysis for everyone," *Remote Sens. Environ.* 202 (2017) 18–27, <https://doi.org/10.1016/j.rse.2017.06.031>.
- [13] F. Samadzadegan, A. Toosi, F. Dadrass Javan, Automatic built-up area extraction by feature-level fusion of Luojia 1–01 nighttime light and Sentinel satellite imageries in Google Earth Engine, *Adv. Sp. Res.* 72 (4) (2023) 1052–1069, <https://doi.org/10.1016/j.asr.2023.05.015>. Aug.
- [14] H. Farhadi, T. Managhebi, H. Ebadi, "Buildings extraction in urban areas based on the radar and optical time series data using Google Earth Engine," *Sci. Q. Geogr. Data* 30 (120) (2022) 43–63.
- [15] A. Ghorbanian, M. Kakooei, M. Amani, S. Mahdavi, A. Mohammadzadeh, M. Hasanlou, "Improved land cover map of Iran using Sentinel imagery within Google Earth Engine and a novel automatic workflow for land cover classification using migrated training samples," *ISPRS J. Photogramm. Remote Sens.* 167 (April) (2020) 276–288, <https://doi.org/10.1016/j.isprsjprs.2020.07.013>.
- [16] M. Amiri, H.R. Pourghasemi, "Mapping the NDVI and monitoring of its changes using google Earth engine and sentinel-2 images," *Comput. Earth Environ. Sci. Artif. Intell. Adv. Technol. Hazards Risk Manag.* (Jan. 2022) 127–136, <https://doi.org/10.1016/B978-0-323-89861-4.00044-0>.
- [17] J. Joiner, et al., "Global relationships among traditional reflectance vegetation indices (NDVI and NDII), evapotranspiration (ET), and soil moisture variability on weekly timescales," *Remote Sens. Environ.* 219 (October) (2018) 339–352, <https://doi.org/10.1016/j.rse.2018.10.020>.
- [18] M. Amani, B. Salehi, S. Mahdavi, A. Masjedi, S. Dehnavi, "Temperature-Vegetation-soil moisture dryness index (TVMDI)," *Remote Sens. Environ.* 197 (2017) 1–14, <https://doi.org/10.1016/j.rse.2017.05.026>.
- [19] N. Arif, P. Danoedoro, A. Mulabbi, "Prediction model using fractional vegetation," *Indones. J. Sci. Technol. Eros* 5 (1) (2020) 125–132.
- [20] Z. Gao, X. Xu, J. Wang, H. Yang, W. Huang, H. Feng, "A method of estimating soil moisture based on the linear decomposition of mixture pixels," *Math. Comput. Model.* 58 (3–4) (2013) 606–613, <https://doi.org/10.1016/j.mcm.2011.10.054>.
- [21] J.C. Han, Y. Huang, H. Zhang, X. Wu, "Characterization of elevation and land cover dependent trends of NDVI variations in the Hexi region, northwest China," *J. Environ. Manage.* 232 (June 2018) (2019) 1037–1048, <https://doi.org/10.1016/j.jenvman.2018.11.069>.
- [22] M. El-Attar, "Evaluating and empirically improving the visual syntax of use case diagrams," *J. Syst. Softw.* 156 (2019) 136–163, <https://doi.org/10.1016/J.JSS.2019.06.096>.
- [23] S. Guha, H. Govil, "An assessment on the relationship between land surface temperature and normalized difference vegetation index," *Environ. Dev. Sustain.* (2020) 0123456789 <https://doi.org/10.1007/s10668-020-00657-6>.
- [24] P. Nwaerema, O.N. Vincent, C. Amadou, A.I. Morrison, "Spatial assessment of land surface temperature and emissivity in the tropical littoral city of port harcourt, Nigeria," *Int. J. Environ. Clim. Chang.* (2019) 88–103, <https://doi.org/10.9734/ijec/2019/v9i230099>. April.
- [25] Q. Weng, "Thermal infrared remote sensing for urban climate and environmental studies: methods, applications, and trends," *ISPRS J. Photogramm. Remote Sens.* 64 (4) (2009) 335–344, <https://doi.org/10.1016/j.isprsjprs.2009.03.007>.
- [26] H. Xu, Analysis on urban heat island effect based on the dynamics of urban surface biophysical descriptors, *Shengtai Xuebao/ Acta Ecol. Sin.* 31 (2011) 3890–3901.
- [27] N. Arif, A. Wardhana, A. Martiana, "Spatial analysis of the urban physical vulnerability using remote sensing and geographic information systems (case study: Yogyakarta City)," *IOP Conf. Ser. Earth Environ. Sci.* 986 (1) (Feb. 2022) 012067 <https://doi.org/10.1088/1755-1315/986/1/012067>.
- [28] B. Roy, E. Bari, "Examining the relationship between land surface temperature and landscape features using spectral indices with Google Earth Engine," *Heliyon* 8 (9) (2022) e10668 <https://doi.org/10.1016/j.heliyon.2022.e10668>.
- [29] M.Y. Yasin, J. Abdullah, N.M. Noor, M.M. Yusoff, N.M. Noor, "Landsat observation of urban growth and land use change using NDVI and NDBI analysis," *IOP Conf. Ser. Earth Environ. Sci.* 1067 (1) (2022) <https://doi.org/10.1088/1755-1315/1067/1/012037>.
- [30] M.S. Malik, J.P. Shukla, S. Mishra, "Relationship of LST, NDBI and NDVI using landsat-8 data in Kandaihimmat watershed, Hoshangabad, India," *Indian J. Geo-Marine Sci.* 48 (1) (2019) 25–31.
- [31] S. Pal, S. Ziaul, "Detection of land use and land cover change and land surface temperature in English Bazar urban centre," *Egypt. J. Remote Sens. Sp. Sci.* 20 (1) (2017) 125–145, <https://doi.org/10.1016/j.ejrs.2016.11.003>.
- [32] K. Jafarpour Ghalehtemouri, A. Shamsoddini, M.N. Mousavi, F. Binti Che Ros, A. Khedmatzadeh, "Predicting spatial and decadal of land use and land cover change using integrated cellular automata Markov chain model based scenarios (2019–2049) Zarrin-Rud River Basin in Iran," *Environ. Challenges* 6 (2022) 100399 <https://doi.org/10.1016/j.envc.2021.100399>.
- [33] S. Dinda, N. Das Chatterjee, S. Ghosh, "An integrated simulation approach to the assessment of urban growth pattern and loss in urban green space in Kolkata, India: a GIS-based analysis," *Ecol. Indic.* 121 (2021) 107178 <https://doi.org/10.1016/j.ecolind.2020.107178>.
- [34] H. Fathizad, N. Rostami, M. Faramarzi, "Detection and prediction of land cover changes using Markov chain model in semi-arid rangeland in western Iran," *Environ. Monit. Assess.* 187 (10) (2015) <https://doi.org/10.1007/s10661-015-4805-y>.
- [35] R. Hamad, H. Balzter, K. Kolo, "Predicting land use/land cover changes using a CA-Markov model under two different scenarios," *Sustain. Times* 10 (10) (2018) 1–23, <https://doi.org/10.3390/su10103421>.
- [36] N. Arif, Y. Susena, "Soil moisture mapping for drought monitoring in urban areas," *IOP Conf. Ser. Earth Environ. Sci.* 1314 (1) (2024) <https://doi.org/10.1088/1755-1315/1314/1/012087>.
- [37] <https://www.severe-weather.eu/>, "Weather 2022: New anomalies are growing in the Atmosphere and the Oceans, that will change the weather patterns as we head deeper into the year," 2022. <https://climatechange.novascotia.ca/>.
- [38] L. Pérez-Domínguez, H. Garg, D. Luviano-Cruz, J.L. García Alcaraz, "Estimation of linear regression with the dimensional analysis method," *Mathematics* 10 (10) (2022) <https://doi.org/10.3390/math10101645>.
- [39] R. Lasaponara, N. Abate, C. Fattore, A. Aromando, G. Cardettini, M. Di Fonzo, "On the use of sentinel-2 NDVI time series and google Earth engine to detect land-use/land-cover changes in fire-affected areas," *Remote Sens.* 14 (19) (2022) <https://doi.org/10.3390/rs14194723>.
- [40] V. Saini, "Mapping environmental impacts of rapid urbanisation and deriving relationship between NDVI, NDBI and surface temperature: a case study," *IOP Conf. Ser. Earth Environ. Sci.* 940 (1) (2021) <https://doi.org/10.1088/1755-1315/940/1/012005>.
- [41] A. Zaitunah, A. Samsuri, F. Silitonga, L. Syaufina, "Urban greening effect on land surface temperature," *Sensors* 22 (11) (2022) 1–14, <https://doi.org/10.3390/s22114168>.
- [42] N. Kikon, D. Kumar, S.A. Ahmed, "Quantitative assessment of land surface temperature and vegetation indices on a kilometer grid scale," *Environ. Sci. Pollut. Res.* 30 (49) (2023) 107236–107258, <https://doi.org/10.1007/s11356-023-27418-y>.
- [43] T.D. Mushore, O. Mutanga, J. Odindi, "Estimating urban LST using multiple remotely sensed spectral indices and elevation retrievals," *Sustain. Cities Soc.* 78 (2022) 103623 <https://doi.org/10.1016/j.scs.2021.103623>.
- [44] P. Chotchaiwong, S. Wijitkosum, "Relationship between land surface temperature and land use in Nakhon Ratchasima city, Thailand," *Eng. J.* 23 (4) (2019) 1–14, <https://doi.org/10.4186/ej.2019.23.4.1>.



- [45] M. Gascon, et al., "Normalized difference vegetation index (NDVI) as a marker of surrounding greenness in epidemiological studies: the case of Barcelona city," *Urban For. Urban Green.* 19 (2016) 88–94, <https://doi.org/10.1016/j.ufug.2016.07.001>.
- [46] P.E. Osgouei, S. Kaya, E. Sertel, U. Alganci, "Separating built-up areas from bare land in mediterranean cities using Sentinel-2A imagery," *Remote Sens.* 11 (3) (2019) <https://doi.org/10.3390/rs11030345>.
- [47] W.G.M. Bastiaanssen, M. Menenti, R.A. Feddes, A.A.M. Holtslag, "1998-Bastiaanssen-surface energy balance algorithm for land (SEBAL): 1. Formulation.PDF," *J. Hydrol.* 213 (1998) 198–212.
- [48] A.R. As-syakur, I.W.S. Adnyana, I.W. Arthana, I.W. Nuarsa, "Enhanced built-UP and bareness index (EBBI) for mapping built-UP and bare land in an urban area," *Remote Sens.* 4 (10) (2012) 2957–2970, <https://doi.org/10.3390/rs4102957>.
- [49] Statistics of Daerah Istimewa Yogyakarta (BPS), Daerah Istimewa Yogyakarta Province in Figures 369 (1) (2022), <https://doi.org/10.1017/CBO9781107415324.004>, 2022.
- [50] H. Lee, N. Kim, S. Kim, Y. Yoon, "Detecting socioeconomic changes of Chicago regions between 2013 and 2020 using urban region representation learning," *Procedia Comput. Sci.* 220 (2023) 259–266, <https://doi.org/10.1016/j.procs.2023.03.034>.
- [51] S. Zhang, et al., "Equalization measurement and optimization of the public cultural facilities distribution in tianjin central area," *Sustainability* 15 (6) (2023) 4856, <https://doi.org/10.3390/su15064856>.
- [52] M.A. Zoran, R.S. Savastru, D.M. Savastru, M.N. Tautan, L.A. Baschir, "Analysis of urbanization and climate change impacts on the urban thermal environment based on MODIS satellite data," in: *Earth Resources and Environmental Remote Sensing/GIS Applications V*, 2014, <https://doi.org/10.1117/12.2067164>.
- [53] S.T.J. Putro, N. Arif, T. Sarastika, "Land surface temperature (LST) and soil moisture index (SMI) to identify slope stability," *IOP Conf. Ser. Earth Environ. Sci.* 986 (1) (2022) <https://doi.org/10.1088/1755-1315/986/1/012022>.
- [54] G. Wang, Q. Zhang, X. Rongbo, D. Guan, "Impacts of Land Use, Population Density and Altitude on the Urban Heat Island," Mar. 2019, <https://doi.org/10.7540/j.ynu.20170584>.
- [55] M. Dushi, A. Berilla, "Determining the influence of population density on the land surface temperature based on remote sensing data and gis techniques: application to prizen, kosovo," *Sci. Rev. Eng. Environ. Sci.* 31 (1) (2022) 47–62, <https://doi.org/10.22630/srees.2324>.
- [56] J. Guo, G. Han, Y. Xie, Z. Cai, Y. Zhao, "Exploring the relationships between urban spatial form factors and land surface temperature in mountainous area: a case study in Chongqing city, China," *Sustain. Cities Soc.* 61 (2020) 102286 <https://doi.org/10.1016/j.scs.2020.102286>.
- [57] S. Khandelwal, R. Goyal, N. Kaul, A. Mathew, "Assessment of land surface temperature variation due to change in elevation of area surrounding Jaipur, India," *Egypt. J. Remote Sens. Sp. Sci.* 21 (1) (2018) 87–94, <https://doi.org/10.1016/j.ejrs.2017.01.005>.
- [58] N. Arif, A.N. Khasanah, R. Jaya, M. Gozan, B. Hendrawan, "The effect of land surface temperature and land use on energy system development in gorontalo city," in: *Journal of Physics: Conference Series*, 2019, <https://doi.org/10.1088/1742-6596/1179/1/012103>.
- [59] D.R.S. Sumunar, N. Arif, B.S. Hadi, K. Endro, "Urban energy modeling using remote sensing approaches," *Int. J. GEOMATE* 19 (75) (2020) 203–208, <https://doi.org/10.21660/2020.75.23161>.
- [60] T. Qiu, C. Song, Y. Zhang, H. Liu, J.M. Vose, "Urbanization and climate change jointly shift land surface phenology in the northern mid-latitude large cities," *Remote Sens. Environ.* 236 (2020) 111477 <https://doi.org/10.1016/j.rse.2019.111477>.
- [61] N. Arif, N. Nayan, "A n Analyze of Urban Temperature Using Energy Balance Algorithm for Land (SEBAL) in Yogyakarta City," 28 (1) (2023) 31–38, <https://doi.org/10.5400/jts.2023.v28i1.31-38>.
- [62] M. Kumari, K. Sarma, R. Sharma, "Using Moran's I and GIS to study the spatial pattern of land surface temperature in relation to land use/cover around a thermal power plant in Singrauli district, Madhya Pradesh, India," *Remote Sens. Appl. Soc. Environ.* 15 (May) (2019) 100239 <https://doi.org/10.1016/j.rsase.2019.100239>.
- [63] A.E. Al-Dousari, A. Mishra, S. Singh, "Land use land cover change detection and urban sprawl prediction for Kuwait metropolitan region, using multi-layer perceptron neural networks (MLPNN)," *Egypt. J. Remote Sens. Sp. Sci.* 26 (2) (2023) 381–392, <https://doi.org/10.1016/j.ejrs.2023.05.003>.
- [64] M.R. Rahnama, "Forecasting land-use changes in Mashhad Metropolitan area using Cellular Automata and Markov chain model for 2016-2030," *Sustain. Cities Soc.* 64 (2021) 102548 <https://doi.org/10.1016/j.scs.2020.102548>.
- [65] T.S.P. Nunna, A. Banerjee, "Impact of tourism on spatial growth of the destination," *Proc. Annu. Int. Conf. Archit. Civ. Eng.*, no. November (2019) 613–617, [https://doi.org/10.5176/2301-394X\\_ACE19.610](https://doi.org/10.5176/2301-394X_ACE19.610).
- [66] A.-A. Faisal, et al., "Assessing and predicting land use/land cover, land surface temperature and urban thermal field variance index using Landsat imagery for Dhaka Metropolitan area," *Environ. Challenges* 4 (2021) 100192, <https://doi.org/10.1016/j.envc.2021.100192>.
- [67] N. Matso, "Analytical study of land surface temperature with NDVI and NDBI using satellite image in baay-licuan, abra, Philippines," *IAMURE Int. J. Ecol. Conserv.* 33 (1) (2020).